RESEARCH ARTICLE | JANUARY 18 2024

Estimation of wintertime cloud radiative effects in the Western Arctic, a function of cloud-moisture-coupling and sea ice conditions

Pablo Saavedra Garfias ; Heike Kalesse-Los; Kerstin Ebell

AIP Conf. Proc. 2988, 070008 (2024)
https://doi.org/10.1063/5.0182751

Estimation of Wintertime Cloud Radiative Effects in the Western Arctic, a Function of Cloud-Moisture-Coupling and Sea Ice Conditions

Pablo Saavedra Garfias,[1, a)] Heike Kalesse-Los,[1, b)] and Kerstin Ebell[2, c)]

[1)] *University of Leipzig, Institute for Meteorology, Faculty of Physics and Geosciences, Leipzig, Germany.*

[2)] *University of Cologne, Institute for Geophysics and Meteorology, Cologne, Germany*

[a)] *Corresponding author: pablo.saavedra@uni-leipzig.de*

[b)] *Electronic mail: heike.kalesse@uni-leipzig.de*

[c)] *Electronic mail: kebell@meteo.uni-koeln.de*

Abstract Cloud radiative effects are estimated using up- and downward ground-based observations of broadband thermal infrared sensors in cloudy conditions which are provided by the ARM data repository. The ARM Surface Radiation measurement is analyzed. To study the cloud radiative effects, the observed thermal infrared measurements under cloudy conditions are analyzed together with microphysical cloud properties like liquid and ice water path obtained from the CloudNet algorithms applied to the remote-sensing instrumentation suite at the ARM site in Utqiaġvik. Cloud observations have been sorted depending on the coupling of the cloud with upwind water vapor transport events that can interact with sea ice upwind. Statistics of surface net thermal fluxes and cloud water/ice properties show a distinguished distribution for coupled and decoupled clouds. It was found that coupled clouds contain more liquid water and are more efficient reduce the cooling of surface LW radiation.

INTRODUCTION

Clouds are a driving element in the Arctic climate system due to their interaction with solar and thermal infrared radiation, yet their contribution to the Arctic amplification is still uncertain. Therefore long-term studies are paramount in order to better understand the Arctic climate system. The Atmospheric Radiation Measurement (ARM) program's North Slope of Alaska (NSA) observational site located in Utqiaġvik, Alaska, is one of the main source for long-term high-quality observations for clouds and radiation studies in the Western Arctic (Fig. 1, left). The present study uses observations from NSA to study cloud radiative effects (CRE) focused on the cloud coupled to water vapour transport that has interacted with different sea ice conditions upwind. We only focus on longwave (LW) radiation. To minimize the influence of solar shortwave (SW) we study Arctic winters (Nov. to Mar.) from 2012 to 2020. The scientific questions to be investigated are three-fold: 1. How are macro- and microphysical cloud properties influenced by the presence of leads or polynyas?, 2. To which extend does the coupling/decoupling of clouds to moisture-layer impact the cloud's radiative properties?, and 3. How do mixed-phase clouds affect CRE for coupled/decoupled cases?

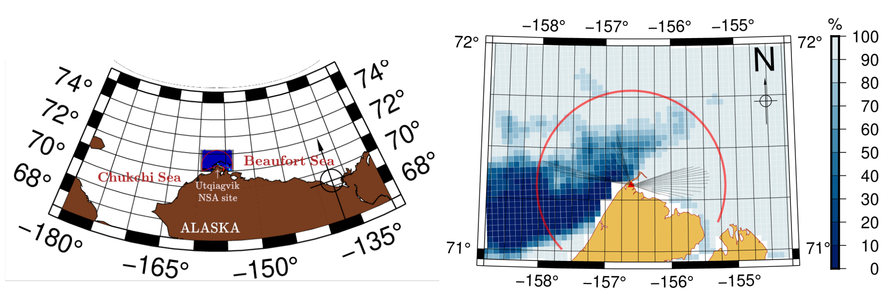

Figure 1. Left: The ARM site in the North Slope of Alaska (71.23° North, 156.61° West) in Utqiaġvik, Alaska. Right: AMSR2 sea ice concentration from 23th March 2019, considered within a 50 km radius (red circle).

Radiation Processes in the Atmosphere and Ocean
AIP Conf. Proc. 2988, 070008-1–070008-4; https://doi.org/10.1063/5.0182751
Published by AIP Publishing. 978-0-7354-4779-0/$30.00

METHODOLOGY

Radiation data from the ARM Radiative Flux Analysis (RADFLUXANAL) [1] comprised of quality controlled broad-band shortwave (SW) and longwave (LW) radiation fluxes is used. In this study only LW fluxes observations are included when the lidar has detected at least one cloud layer.

***S**ea ice concentration:* Sea ice data are obtained from daily satellite retrievals provided by the University of Bremen public repository (www.seaice.uni-bremen.de). The product used is the AMSR2 sea ice (ASI) concentration at a grid resolution of 3.124 km as shown in Fig. 1 (right panel). We consider SIC within a sector of radius of 50 km centered around NSA. For the following analysis, only SIC from grid pixels which are located at the direction of the maximum gradient of water vapour transport are considered, for example the grey lines in Fig. 1 right panel.

Sea ice - atmosphere coupling conceptual model: The following analysis is performed to couple sea ice conditions upwind with cloud observations above NSA. The vertical gradient of water vapour transport ($\nabla_z WVT$) is calculated from radiosonde humidity and wind profiles. The direction of maximum $\nabla_z WVT$ (see grey lines in Fig. 1) is used as a means to relate SIC with the observed clouds at NSA. The physical reason to use $\nabla_z WVT$ as couple mechanism for sea ice condition and clouds is that the open sea ice areas are effective sources of heat and moisture which are transported by the wind towards the observatory, this moisture interaction with the cloud is the basis of this study. To classify cases where the WVT is coupled or decoupled to the cloud, the cumulative variance of virtual potential temperature θ_v is analyzed from the cloud base height downwards to an altitude where the variance exceeds a certain threshold. That altitude is assigned as mixing cloud layer below cloud base. If the maximum of $\nabla_z WVT$ is located within this layer and cloud top, the cloud is assigned to be coupled, otherwise decoupled. This technique has been developed and applied to NSA by [2].

Skin temperature estimation considering SIC: The surface skin temperature is calculated based on an empirical function (1) that relates SIC with the surface temperature calculated from the up-welling and down-welling LW flux.

$$T_{skin}(\mathtt{SIC}, T_s) = \mathtt{SIC} \times T_s \, + \, (1 \, - \, \mathtt{SIC}) \times SST \tag{1}$$

with SST being sea surface temperature (assumed 271.34 K), SIC ranging from $0 \dots 1$, and T_s the surface temperature derived from flux observations given by Eq. 2. T_{skin} tends to SST when SIC approaches zero, otherwise is T_s given by:

$$T_s = \left[\frac{F_{lw}^{\uparrow} - (1 - \varepsilon_s) F_{lw}^{\downarrow}}{\varepsilon_s \, \sigma} \right]^{\frac{1}{4}} \tag{2}$$

with $F_{lw}^{\downarrow}$ and $F_{lw}^{\uparrow}$ being down- and up-welling measured LW fluxes [3, 4]. The surface LW emissivity ε_s is assumed to be 0.981±5% as range of characteristic ε_s reported by [5, 6] for NSA winter, and σ the Stephan-Boltzmann constant.

Cloud properties: The cloud macro- and microphysical properties have been derived using the Cloudnet classification algorithm in its open source version (Cloudnetpy) developed by [7]. The input of Cloudnet processing chain consists of ground-based remote sensing cloud radar, lidar and microwave radiometer. The input data have been obtained from the NSA site observations and pre-processed to Cloudnet input format by [2]. Main Cloudnet outputs used in this study are the path integrated liquid water (LWP) and ice water content (IWP).

RESULTS

Surface long-wave net radiation fluxes are analyzed as function of e.g. liquid and ice water path (LWP, IWP), skin temperature based on SIC, and cloud mixed-phase fraction. Figure 2 (panels A and B) summarizes the distributions of surface net LW flux F_{lw}^{net} versus LWP for coupled (left column) and decoupled (right column) clouds. Coupled clouds produce a F_{lw}^{net} with a mono-modal distribution with maximum occurrence around -10 $\mathtt{W\,m^{-2}}$. On the contrary, decoupled clouds contain less liquid water and their F_{lw}^{net} has a distinguished bi-modal distributions with peaks around -8 and -40 $\mathtt{W\,m^{-2}}$, both F_{lw}^{net} peaks are also characterized by a wider spread around them. This result suggests that coupled cloud are characterized by a higher liquid water content and they are more effective in balancing the surface net LW fluxes, i.e. the down-welling component is stronger to countervail the surface up-welling radiation. This is not the case for decoupled clouds.

Since the sensible heat flux is proportional to the temperature difference at the interface between surface and the adjacent atmospheric layer, a relationship between the sensible heat flux and the net LW flux can be studied. To do so we define ΔT as the temperature difference given by Eq. 3.

$$\Delta T \; = \; T_{skin}(\mathtt{SIC}, T_s) \; - \; T_{2m} \tag{3}$$

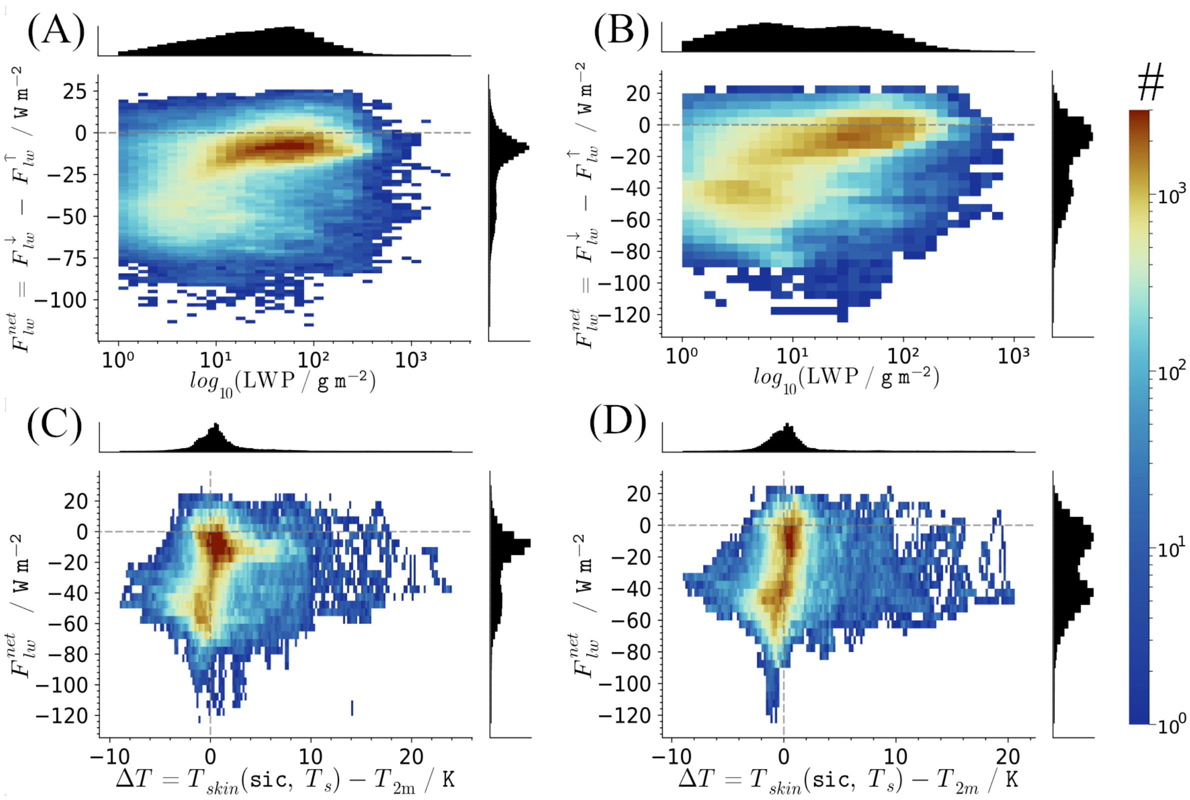

Figure 2. Top row: Distributions for surface net LW radiation F_{lw}^{net} versus LWP for coupled (A) and decoupled (B) cases. Bottom row shows surface net LW radiation versus ΔT defined in Eq. 3 for coupled (C) and decoupled (D) clouds.

with T_{2m} is the standard two meter air temperature and $T_{skin}(\mathtt{SIC}, T_s)$ is given by Eq. 1.

In Fig. 2 bottom row, the distribution of ΔT as defined by Eq. 3 is used as proxy for SIC dependent sensible heat flux and related with the F_{lw}^{net} for coupled [C] and decoupled [D] cases. It can be seen that most of the ΔT data are concentrated around zero with a spread of about ± 2 K, meaning the surface and lowest atmosphere layer are close to thermodynamic equilibrium. The long positive skewed tail of ΔT is produced by cases with low SIC, however as the distribution clearly shows, these cases have a low frequency of occurrence and most of the data are associated to SIC above 85%. The decoupled case Fig. 2 [D] shows even clearer the bi-modal feature of the F_{lw}^{net} distribution when sorted by ΔT.

Analyzing the F_{lw}^{net} with respect to the fraction of liquid/ice water path as depicted in Fig. 3 (left), shows that coupled mixed-phase clouds are more effective to decrease the amount of LW surface cooling compared to decoupled mixed-phase clouds. Note a difference of up to 10 W m^{-2} for a fraction of $\sim$0.35. When sees the effect of ice cloud water path (Fig. 3, right) coupled clouds systematically decrease the surface cooling regardless the IWP magnitude.

Moreover it is interesting to note from Fig. 3 (left) that for coupled cases the effectiveness of mixed-phase clouds in warming the surface at LW radiation is mostly observable for liquid/ice fraction below 0.5, whereas for cases when the cloud is mostly liquid there is no clear difference in F_{lw}^{net} between coupled and decoupled cases. This might be related to the total water content in the mixed-phase cloud or the presence of multi-layer clouds and needs to be studied more deeply.

CONCLUSIONS

Surface thermal radiation observations at the ARM NSA site have been analyzed for the wintertime period 2012 to 2020. The data have been classified into cloud-water vapour transport coupled/decoupled cases with sea ice conditions upwind. Results are summarized as:

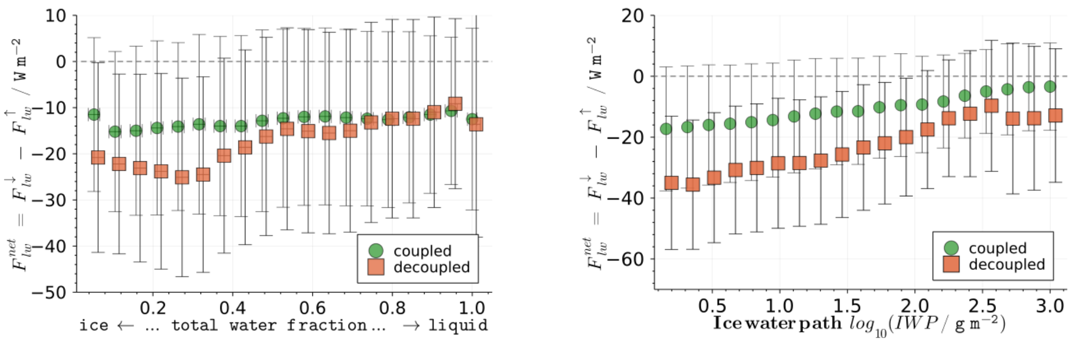

Figure 3. Net LW flux versus cloud phase fraction (left) and ice water path (right) for coupled (green circles) and decoupled (orange squares) clouds. IWP is calculated using retrievals obtained from the Cloudnet algorithm.

- F_{lw}^{net} has a mono-modal and bi-modal distribution for coupled and decoupled cases respectively. This can be related to the finding that decoupled cases are mostly comprised of high level clouds which might comprise of low cloud fraction allowing clear-sky patches to reach the LW sensor,
- Coupled clouds are more effective to diminish the surface thermal cooling (less negative F_{lw}^{net}),
- Mixed-phase cloud properties (with varying ratios of LWP and IWP) shown that for coupled clouds with liquid below 50% the F_{lw}^{net} can reduce the surface cooling in average by up to 10 $\mathrm{W\,m^{-2}}$.

Results are consistent with [2] on the effect of leads or polynyas on cloud properties, but contradictory to [8] who claims high lead fraction (i.e. low SIC values) reduces pre-existing low level clouds that in turn decreases downwelling thermal flux, accelerating the freezing of sea ice. No direct hint to support that claim has been found, and this apparent discrepancies need to be further researched.

To achieve a complete picture, we will include the cloud radiative effects (CRE) which is defined as the difference between the net all-sky and clear-sky fluxes following the same methodology as [4] successfully applied to the central Arctic site Ny Ålesund, Svalbard.

ACKNOWLEDGMENTS

This work is supported by the DFG funded Transregio-project TR-172 "Arctic Amplification $(AC)^3$". Thanks to ARM program and the University of Bremen under supported by Dr. Gunnar Spreen for providing SIC data.

REFERENCES

1. L. D. Riihimaki, K. L. Gaustad, C. N. Long, and PNNL, BNL, ANL, ORNL, “Radiative Flux Analysis (RADFLUXANAL) Value-Added Product: Retrieval of Clear-Sky Broadband Radiative Fluxes and Other Derived Values,” http://www.osti.gov/servlets/purl/1569477/ (2019), 10.2172/1569477.
2. P. Saavedra Garfias, H. Kalesse-Los, and W. Schimmel, “Climatology of clouds containing supercooled liquid in the Western and central Arctic,” Earth and Space Science Open Archive , 5 (2021), https://doi.org/10.1002/essoar.10509918.1.
3. G. Thakur, S. J. Schymanski, K. Mallick, I. Trebs, and M. Sulis, “Downwelling longwave radiation and sensible heat flux observations are critical for surface temperature and emissivity estimation from flux tower data,” Scientific Reports **12** (2022), 10.1038/s41598-022-12304-3.
4. K. Ebell, T. Nomokonova, M. Maturilli, and C. Ritter, “Radiative Effect of Clouds at Ny-Ålesund, Svalbard, as Inferred from Ground-Based Remote Sensing Observations,” Journal of Applied Meteorology and Climatology **59** (2020), 10.1175/JAMC-D-19-0080.1.
5. M. D. Shupe, D. D. Turner, A. Zwink, M. M. Thieman, E. J. Mlawer, and T. Shippert, “Deriving Arctic Cloud Microphysics at Barrow, Alaska: Algorithms, Results, and Radiative Closure,” Journal of Applied Meteorology and Climatology **54** (2015), 10.1175/JAMC-D-15-0054.1.
6. E. K. Dolinar, X. Dong, B. Xi, J. H. Jiang, and N. G. Loeb, “A clear-sky radiation closure study using a one-dimensional radiative transfer model and collocated satellite-surface-reanalysis data sets,” Journal of Geophysical Research: Atmospheres **121**, 13,698–13,714 (2016), _eprint: https://onlinelibrary.wiley.com/doi/pdf/10.1002/2016JD025823.
7. S. Tukiainen, E. O’Connor, and A. Korpinen, “CloudnetPy: A Python package for processing cloud remote sensing data,” Journal of Open Source Software **5**, 2123 (2020).
8. X. Li, S. K. Krueger, C. Strong, G. G. Mace, and S. Benson, “Midwinter Arctic leads form and dissipate low clouds,” Nature Communications **11**, 206 (2020), DOI:10.1038/s41467-019-14074-5.
9. W. Brutsaert, “On a derivable formula for longwave radiation from clear skies,” Water Res. Resch. **3**, 742–744 (1975).
10. C. N. Long and D. D. Turner, “A method for continuous estimation of clear-sky downwelling longwave radiative flux developed using ARM surface measurements,” Journal of Geophysical Research: Atmospheres **113** (2008), 10.1029/2008JD009936.